

# Measurement of Absorbed Dose Rate in Air at NIFS Site after the First Deuterium Plasma Experiment in LHD

Yoshitaka SHIROMA, Shigekazu HIRAO<sup>1)</sup>, Naofumi AKATA<sup>2)</sup>, Masahide FURUKAWA, Hitoshi MIYAKE<sup>3)</sup>, Hiroshi HAYASHI<sup>3)</sup>, Takuya SAZE<sup>3)</sup> and Masahiro TANAKA<sup>3)</sup>

*University of the Ryukyus, Nishihara, Okinawa 903-0213, Japan*

<sup>1)</sup>*Fukushima University, Kanayagawa, Fukushima 960-1296, Japan*

<sup>2)</sup>*Hirosaki University, Hirosaki, Aomori 036-8564, Japan*

<sup>3)</sup>*National Institute for Fusion Science, Toki, Gifu 509-5292, Japan*

(Received 8 May 2019 / Accepted 5 June 2019)

The latest measurement of the absorbed dose rate in air was performed at the National Institute for Fusion Science (NIFS) site during the period for the first deuterium plasma experiment conducted in Large Helical Device (LHD). The arithmetic mean of the absorbed dose rates in air for 222 measurement points at the NIFS site was 43 nGy h<sup>-1</sup>. Very little change was observed in the distribution maps of the absorbed dose rates in air before and after the deuterium experiment in the LHD. In addition, the absorbed dose rates in air around the buildings were distributed at similar high levels before and after the deuterium experiment. A radionuclide analysis of soil and broken stone was conducted using a high-purity Ge semiconductor detector. The absorbed dose rates in air at the NIFS site were mainly defined by the radiation from the ground and the building material around the measurement points. The effect of the deuterium experiment was so small that it was undetectable in this study.

© 2019 The Japan Society of Plasma Science and Nuclear Fusion Research

Keywords: absorbed dose rate in air, environmental radiation, background measurement, deuterium plasma experiment, NIFS site

DOI: 10.1585/pfr.14.1305130

The National Institute for Fusion Science (NIFS) has initiated the deuterium experiment in Large Helical Device (LHD). In a deuterium experiment, neutrons and tritium are generated through a D–D reaction. The deuterium plasma experiments in the LHD were performed considering the annual neutron yield and amount of tritium production [1, 2]. From the perspectives of worker safety and public acceptance of radiation experiments, the produced tritium was recovered using an exhaust detritiation system, which has a tritium recovery performance of more than 95% [3]. Additionally, the neutrons were shielded by a 2-m-thick concrete wall. Although the effect of neutrons and tritium is reduced using such precautions, monitoring the radiation around the fusion test facility is important to ensure environmental safety. Tritium monitoring around the NIFS site was conducted prior to performing the deuterium plasma experiment [4–6]. Further, radiation monitoring of the NIFS site was performed using glass dosimeters and a radiation monitoring system applicable to fusion experiments [7]. The radiation distribution was evaluated in detail for the NIFS site and the effects of the deuterium plasma experiment were confirmed by measuring the absorbed dose rate in air before the experiments were conducted [8]. In this previous study [8], the absorbed dose rates in the air near the building were reported to be rel-

atively high. However, absorbed dose rates in air tend to be low away from buildings. Thus, building materials may enhance the absorbed dose rate in air. The present study investigates changes in the absorbed dose rate in air before and after the first deuterium experiments were performed in addition to the main factors that contributed to the absorbed dose rates in air at the NIFS site.

NIFS is located in Toki City, Gifu Prefecture, Japan (Fig. 1). Figure 2 shows a map of the NIFS site. The NIFS site area is approximately 464,000 m<sup>2</sup>. An LHD building is on site a little east of the center. The site, excluding roads, parking, and buildings, is managed as a forest reserve and a green district.

A pocket survey meter containing a CsI(Tl) scintillator (PDR-101, Hitachi Ltd., Japan) was used to measure the dose at multiple points over a short period. The measurement ranges for a 1-cm dose equivalent rate and the energy characteristic were 0.001 to 19.99 μSv h<sup>-1</sup> and 60 keV to 1.25 MeV, respectively. The instrument was held at a height of approximately 1 m, and a display value of 2 or more significant figures was read using the accuracy enhancing mode. Variations in the display values of the instrument were evaluated by performing 15 measurements at a single point. The 1-cm dose equivalent rates (μSv h<sup>-1</sup>) that were obtained by the instrument were converted to the absorbed dose rate in air (nGy h<sup>-1</sup>) using a previously ob-

author's e-mail: tanaka.masahiro@nifs.ac.jp

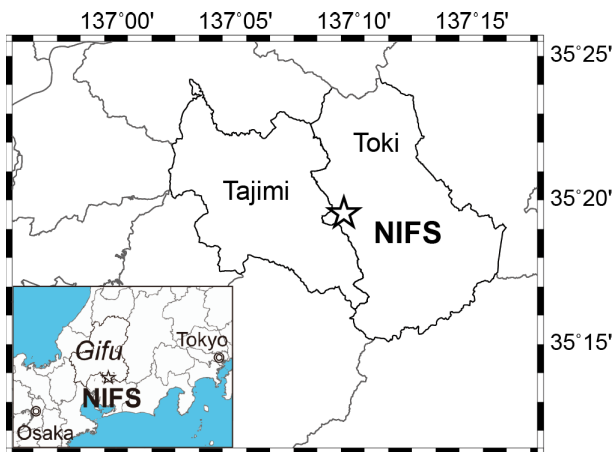


Fig. 1 Location of the National Institute for Fusion Science (NIFS) site.

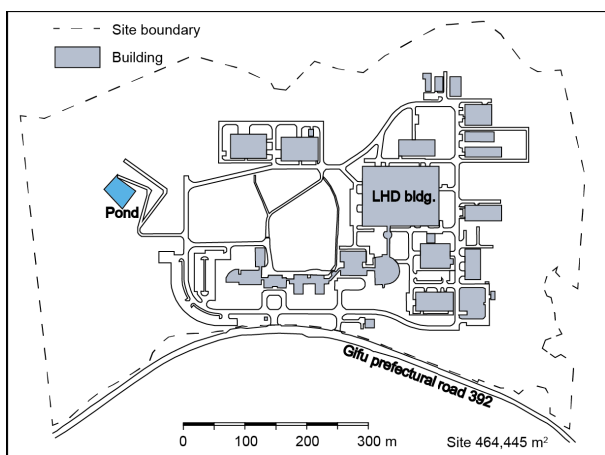


Fig. 2 NIFS physical site map.

tained conversion factor (711.9) [8]. The latitude and longitude of each measurement point were also recorded using a handheld global positioning system device (eTrex 10J, Garmin Ltd., Switzerland). In addition, the land use classification at each measurement point was recorded via observation. A distribution map of the absorbed dose rate in air was drawn using generic mapping tools [9]. The origin of the radiation was determined by collecting soil and multiple pieces of broken stone at the NIFS site. The soil was original to the NIFS site and was taken from a location with a low absorbed dose rate in air on the east side of the site. The stone was collected from a location with a high absorbed dose rate in air on the west side of the NIFS site. The samples were dried and pulverized, and then sealed in airtight cylindrical polypropylene containers ( $\varphi 48 \text{ mm} \times \text{H}55 \text{ mm}$ ). The airtight containers were stored for 40 days until  $^{226}\text{Ra}$  and  $^{222}\text{Rn}$  attained radioactive equilibrium. The radioactive nuclides in these samples were analyzed using a high-purity Ge detector (GX3518, Mirion Technologies (Canberra) KK, Japan) with an 80,000-s measurement

time. The photopeaks for  $^{214}\text{Pb}$  at 352 keV and  $^{214}\text{Bi}$  at 609 keV were used to estimate the  $^{238}\text{U}$  series concentration. The  $^{228}\text{Ac}$  photopeak at 911 keV was used to estimate the  $^{232}\text{Th}$  series concentration. The  $^{40}\text{K}$  concentration was also determined based on its single photo peak at 1,461 keV.

The measurements for absorbed dose rate in air were performed at 222 points during the first deuterium experiment from October 24, 2018 to November 30, 2018. The weather conditions were either sunny or cloudy throughout the entire measurement period. The range (arithmetic mean  $\pm$  standard deviation) of the absorbed dose rate in air using the 222 points was 20–74 ( $43 \pm 13$ )  $\text{nGy h}^{-1}$ . The range of 15 measurements at the same point which were separate from 222 measurements was 62–73 ( $65 \pm 3$ )  $\text{nGy h}^{-1}$ . The relative sample standard deviation was 5%, which was considered as the uncertainty in a one-time measurement of a 1-cm dose equivalent rate. This uncertainty was the same as or slightly higher than that of a one-time measurement for absorbed dose rate in air using a  $3 \times 3$ -inch NaI(Tl) scintillation spectrometer (EMF-211, EMF-Japan, Japan). Here, the uncertainty was assumed to be 5% to avoid underestimation of the uncertainty. The uncertainty in the conversion factor was considered as the relative standard error (2.7%) in the estimation coefficient of the linear regression model. The uncertainty in the distance between the instrument and the ground was estimated to be approximately 5%. Assuming that these relative uncertainties were independent of each other and are synthesized by the sum of squares, the combined relative uncertainty was approximately 9%. Therefore, the extended relative uncertainty ( $k = 2$ ) was 18%. However, considering that the uncertainty increases when a sufficient count cannot be obtained for a low dose rate, the extended uncertainty ( $k = 2$ ) in the measurement method performed in this study was estimated to be approximately 18% to 20%.

Figure 3 shows the relative frequency distribution of the absorbed dose rate in air. The relative frequency distribution exhibited two peaks with apexes of approximately 55 and 30  $\text{nGy h}^{-1}$ . Comparing the density curves before and after the deuterium experiment revealed that the relative frequencies were different because the total number of measurement points was different. However, two peaks were observed at the same absorbed dose rate in air. This result suggests that there was little change in the distribution of the absorbed dose rate in air before and after the deuterium experiment.

The distribution of the absorbed dose rate in air is shown in Figs. 4 and 5. These maps were drawn assuming that there were no buildings between the measurement points; i.e., the results were interpolated considering that there were no buildings between the measurement points. The absorbed dose rate in air was high around the buildings, roads, and parking, similar to the results of the previous study [8]. In addition, the absorbed dose rates in air were low for the forest reserve and the green district. The

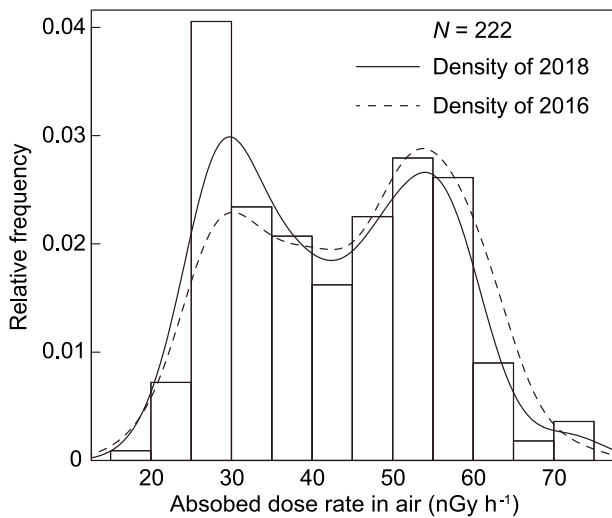


Fig. 3 Histogram of the absorbed dose rate in air at the NIFS site: the black and dotted lines show the densities measured during the deuterium experiments performed in 2018 and before the experiments in 2016, respectively.

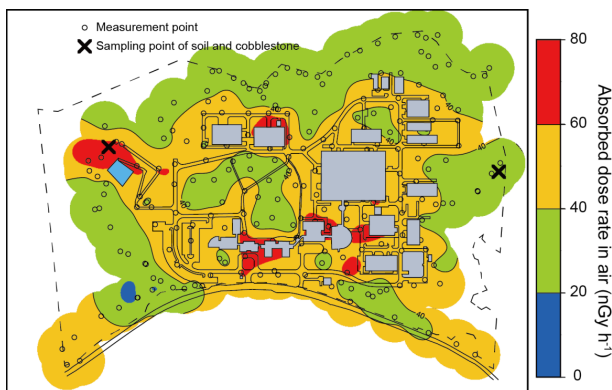


Fig. 4 Map of the distribution of the absorbed dose rate in air at the NIFS site after the first deuterium experiment was performed in the large helical device.

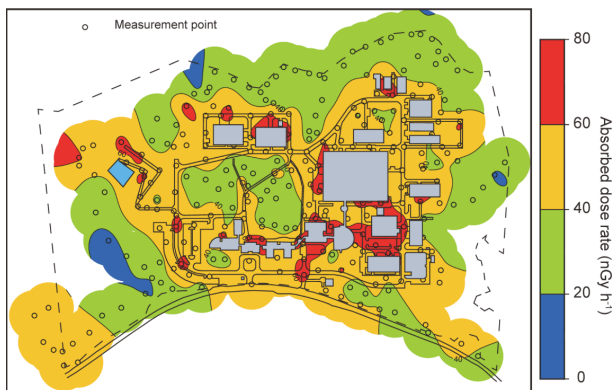


Fig. 5 Map of the distribution of the absorbed dose rate in air at the NIFS site before the deuterium experiment was performed in the LHD [8].

Table 1  $^{238}\text{U}$  series,  $^{232}\text{Th}$  series, and  $^{40}\text{K}$  concentrations for soil and broken stone; corresponding sampling points are shown in Fig. 4.

Sample	Concentration ( $\text{Bq kg}^{-1}$ )		
	$^{238}\text{U}$ series	$^{232}\text{Th}$ series	$^{40}\text{K}$
Soil	$17.7 \pm 0.3$	$19.0 \pm 0.4$	$137 \pm 4$
Broken stone	$28.0 \pm 0.3$	$45.7 \pm 0.6$	$902 \pm 8$

measured absorbed dose rate in air in the present study exhibited variation in some locations compared with the previous study (Fig. 5) [8]. However, this is a reasonable variation considering the uncertainty (18% - 20%) that was evaluated in this study. The measurement points were classified based on land use as belonging to natural and artificial localities. The arithmetic means  $\pm$  standard deviation of the artificial locality ( $n = 110$ ) and the natural locality ( $n = 122$ ) were calculated to be  $52 \pm 8$  and  $35 \pm 10 \text{ nGy h}^{-1}$ , respectively. These values did not change from the mean values for both the artificial ( $55 \pm 6 \text{ nGy h}^{-1}$ ) and natural localities ( $36 \pm 10 \text{ nGy h}^{-1}$ ) obtained in the previous study [8].

Activation nuclides (e.g.,  $^{60}\text{Co}$ ) generated in reactions with neutrons were not detected using the measurement method used in this study for the soil and broken stone. Table 1 shows the detected natural radionuclide concentrations for the soil and broken stone. The  $^{238}\text{U}$  series,  $^{232}\text{Th}$  series, and  $^{40}\text{K}$  concentrations in soil were measured to be  $17.7 \pm 0.3$ ,  $19.0 \pm 0.4$ , and  $137 \pm 4 \text{ Bq kg}^{-1}$ , respectively. The corresponding broken stone concentrations were measured to be  $28.0 \pm 0.3$ ,  $45.7 \pm 0.6$ , and  $902 \pm 8 \text{ Bq kg}^{-1}$ , respectively. The  $^{238}\text{U}$  series,  $^{232}\text{Th}$  series, and  $^{40}\text{K}$  concentrations for broken stone were 2 to 6 times higher than those for soil. Herein, the absorbed dose rate in air was estimated from the radionuclide concentrations in soil and broken stone using the following equation [10]:

$$D = 0.462C_U + 0.604C_{Th} + 0.0417C_K,$$

where  $D$  ( $\text{nGy h}^{-1}$ ) is the gamma-ray dose rate in air at 1 m above the sample surface with a semi-infinite extension and  $C_U$ ,  $C_{Th}$ , and  $C_K$  are the  $^{238}\text{U}$  series,  $^{232}\text{Th}$  series, and  $^{40}\text{K}$  concentrations ( $\text{Bq kg}^{-1}$ ), respectively. Thus, the absorbed dose rates in air ( $D$ ) for soil and broken stone were estimated to be 25 and  $78 \text{ nGy h}^{-1}$ , respectively. These estimated values were in fairly good agreement with the measured values near the sampling points (soil:  $31 \pm 6 \text{ nGy h}^{-1}$ ; broken stone:  $61 \pm 12 \text{ nGy h}^{-1}$ ). This result was obtained because the absorbed dose rates in air at the natural locality were low owing to low radiation from the natural radionuclides in the soil. An alternative explanation is that the absorbed dose rates in air at the artificial locality increased owing to the presence of the broken stone used in the building's foundation. Thus, the absorbed dose rates in air at the

NIFS site were dominated by the radiation from the ground and the building material around the measurement points. The effect of the first deuterium experiment was so small that it was undetectable by this study.

This study was supported by NIFS grant number NIFS18KLEA037.

- [1] M. Osakabe *et al.*, IEEE Trans. Plasma Sci. **46**, 2324 (2018).
- [2] M. Osakabe *et al.*, Fusion Sci. Technol. **72**, 199 (2017).
- [3] M. Tanaka *et al.*, Fusion Eng. Des. **127**, 275 (2018).
- [4] N. Akata *et al.*, Plasma Fusion Res. **11**, 1305032 (2016).
- [5] N. Akata *et al.*, Radiat. Prot. Dosimetry **167**, 210 (2015).
- [6] M. Tanaka and T. Uda, Radiat. Prot. Dosim. **167**, 187 (2015).
- [7] <http://sewhite.nifs.ac.jp/index.html> [in Japanese].
- [8] Y. Shiroma *et al.*, Plasma Fusion Res. **12**, 130529 (2017).
- [9] P. Wessel and W. Smith, Eos. Trans. AGU **72**, 441 (1991).
- [10] H.L. Beck *et al.*, USAEC Repot HASL-258, 10014 (1972).